

Design of high-efficiency microinverter for a photovoltaic system with low harmonic distortion

Walter Naranjo Lourido, Jhon Manuel Sanchez Fierro, Diana Paola Monroy Cadena,
Javier Eduardo Martínez Baquero

Engineering School, Faculty of Basic Sciences and Engineering, Universidad de los Llanos, Villavicencio, Colombia

Article Info

Article history:

Received Aug 6, 2024

Revised Mar 19, 2025

Accepted Jul 4, 2025

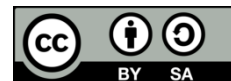
Keywords:

Efficiency
Micro inverter
MPPT
Pure wave
Regulator
Solar panel

ABSTRACT

This article presents the design of a modular pure sine wave microinverter with a high-efficiency maximum power point tracking (MPPT) regulator for photovoltaic (PV) systems. The design starts with a DC/DC buck-boost chopper regulator, simulated using the perturb and observe (P&O) algorithm. Next, a high-frequency DC/AC conversion stage is implemented using a toroidal transformer to achieve various voltage levels and isolated power sources. Finally, a 27-level multilevel inverter is designed to produce a pure sine wave with minimal total harmonic distortion (THD). Simulation results indicate that the microinverter achieves a total efficiency of 90% and produces a pure wave output with 3% harmonic distortion. Compared to commercial solutions, the proposed design enhances efficiency while integrating key components. Additionally, the system maintains a cost-effectiveness and directly proportional to its energy efficiency, making it a viable and cost-effective solution for PV energy conversion.

This is an open access article under the [CC BY-SA](#) license.



Corresponding Author:

Walter Naranjo Lourido

Engineering School, Faculty of Basic Sciences and Engineering, Universidad de los Llanos

Km 12 Via Puerto Lopez. Vereda Barcelona, Villavicencio, Colombia

Email: wnanranjo@unillanos.edu.co

1. INTRODUCTION

Electricity is fundamental to modern infrastructure, powering industries, healthcare, education, and daily life. A reliable energy supply is essential for economic growth, technological advancement, and system stability. Without it, productivity ceases, disrupting critical services and industrial operations. As global energy demand continues to rise, optimizing consumption and integrating sustainable energy sources is imperative for both efficiency and environmental sustainability [1].

Power generation relies on renewable and non-renewable sources, with electricity consumption directly reflecting energy demand. Coal, natural gas, and oil remain dominant but are finite, costly to extract, and environmentally damaging. Their continued use accelerates resource depletion and climate change, reinforcing the urgency of transitioning to cleaner, more sustainable alternatives [2], [3].

Renewable energy technologies provide a clean, abundant, and sustainable solution, minimizing environmental impact while enhancing energy security and long-term economic resilience. Large-scale adoption of renewables reduces dependence on fossil fuels establishing a more resilient energy system [4].

A variety of renewable energy sources serve as viable alternatives to fossil fuels [5], [6]. Unlike centralized power grids, these sources can be integrated into localized microgrid systems, reducing infrastructure requirements and expanding electricity access to remote areas. Selecting the optimal renewable energy source depends on regional resource availability, ensuring efficient and cost-effective implementation [7].

Despite technological advancement, 860 million people will still lack electricity by 2030 if there is no ramp-up in the use of clean energy. This gap in energy affects economic development, health, and education, limiting opportunities in developing regions. Expanding renewable energy infrastructure is essential to universal electricity access [8], [9], while reducing fossil fuel dependence and limiting the environmental harm of greenhouse gas emissions [10], [11].

Use of Photovoltaic systems (PVS) allows for the harvesting of solar energy and its conversion into usable electrical power, offering a viable means of powering different applications. Grid-connected PVS and stand-alone PV power generation have been widely studied for their ability to be implemented for diverse energy needs [12] micro inverter systems (MIS) have further developed in the area of energy efficiency by incorporating boost-half-bridge DC-DC converters and full-bridge pulse-width modulated inverters to achieve maximum power conversion [13]. Recent innovations in microinverter technology have introduced active-clamp step-up DC-DC converters with series-resonant voltage doublers, combined with high-efficiency inverters featuring single-switch-modulation step-down converters [14]. These advancements enhance energy efficiency, improve voltage regulation, and reduce harmonic distortion, making solar energy systems more reliable and effective. Additionally, mass production and technological progress have lowered manufacturing costs, increasing accessibility and affordability for broader adoption.

This project aims to develop a modular pure sine wave microinverter with an integrated high-efficiency, low-cost maximum power point tracking (MPPT) controller to maximize power extraction and improve energy conversion [15]-[18]. The system is built for cost efficiency, scalable, and adaptable to different PV applications, ensuring higher efficiency and seamless grid integration.

To optimize power output, this study employs the disturb and observe (D&O) algorithm for MPPT. This method dynamically adjusts the operating voltage (V_p) based on power fluctuations. If power output increases after a voltage change, the system keeps adjusting in the same direction, but if power decreases, it reverses the voltage perturbation to sustain operation at the maximum power point (MPP). This iterative process ensures optimal energy transfer under varying solar conditions [19]. Figure 1 shows the D&O-based MPPT implementation that establishes the control logic that increases the microinverter efficiency and responsiveness to immediate changes in solar input conditions.

Environmental regulations around the globe increasingly promote the utilization of renewable energy systems through tax incentives and regulatory policy. In Colombia, the national government enacted Decree 829 of 2020, which modifies and complements regulations such as Law 1715 of 2014, Decree 625 of 2016, and Decree 1073, to stimulate investment in non-conventional energy projects [20]. The incentives are aimed at accelerating the transition to sustainable energy solutions, facilitating the use of solar PV systems and other clean energy technologies.

This research aims to provide technical insights into designing more efficient microinverters with lower harmonic distortion. It focuses on developing a microinverter for solar panels that optimally harness solar radiation. The proposed design offers several comparative technical advantages, enhancing energy efficiency. The article is divided into four sections. The introduction outlines the state of the art and research objective. The methodology describes the design characteristics. The results and discussion section examines system performance, simulations, and multilevel inverter features. Lastly, the conclusions highlight key findings.

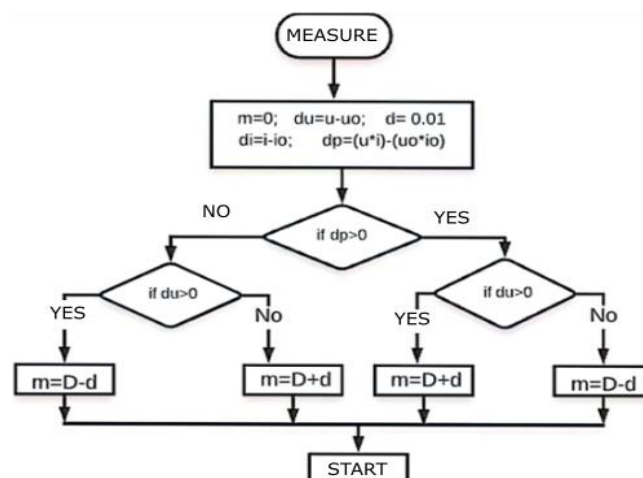


Figure 1. D&O diagram

2. METHOD

The proposed design microinverter system consists of three key components: a DC booster, an HFL inverter, and a multilevel inverter. The topology is designed for maximum power retrieval, high conversion efficacy, and low total harmonic distortion (THD) for PV application. The designing process follows a formalized design process with optimization of the performance of each component, minimization of power losses, and grid integration with no compatibility problems.

The first stage of the system is a DC booster converter that does impedance matching as well as voltage regulation. The booster is designed to change the impedance provided to the solar panel so that it allows MPPT through an adaptive control algorithm such as perturb and observe (P&O). In addition, it increases the panel voltage to the required level, delivering stable and efficient power to the inverter. High-frequency mosfets are used in order to minimize power losses by reducing conduction and switching losses. The MPPT algorithm controls the boost converter, continuously adjusting the duty cycle based on real-time voltage and current measurements to maximize power extraction from the PV panel under varying irradiance conditions.

After voltage regulation, the amplified DC voltage is supplied to a 20 kHz high-frequency link (HFL) inverter, which enhances energy conversion efficiency and offers galvanic isolation between input and output. The HFL topology is extremely useful to overall system performance by reducing the size of passive components and core losses, thus making it a prominent design feature in compact high-efficiency power systems. A high-frequency toroidal transformer is used due to its low hysteresis losses and high efficiency rate (more than 95%), with low energy dissipation [21], [22]. The AC voltages at some ratios (1:3 and 1:9) are generated by this transformer, which are utilized for rectification by Schottky or SiC diodes, with added efficiency and reducing switching losses. The toroidal transformer offers better technical advantages as well, including voltage flexibility, reduced eddy current loss, and electrical isolation [21], [22]. However, to ensure optimal efficiency, copper and core losses must be controlled with caution [23]. To ensure optimal performance, isolated supplies are included in the circuit, with electrical isolation from the rest of the system [24]. This is achieved by summing the voltage in the main and auxiliary sections in the multilevel inverter, thus ensuring power distribution, voltage regulation optimized, and a general compact and efficient structure.

This method gives a step-by-step process of design and implementation of a high-efficiency microinverter with DC booster, HFL, and multilevel inverter. Combining MPPT algorithms, enhanced modulation schemes, and optimized switching of semiconductors, the system is capable of delivering enhanced energy conversion, low THD, and efficient grid integration. Further improvements, such as soft-switching techniques, transformer core design optimization, and real-time adaptive control, can further refine overall performance, and this microinverter system is thus a next-generation technology for distributed PV energy applications.

2.1. Design parameters

The design principles for this project are presented in Table 1. It is MPPT regulator disturb and observe. For optimal efficiency, each solar panel within the system possesses a unique microinverter such that there is maximum power transfer with minimum loss due to mismatching or shading effect. This system enhances the overall energy efficiency of the PV system since it facilitates module-level power conversion and stand-alone MPPT. The proposed microinverter topology is designed to optimize energy harvesting, improve grid compatibility, and reduce power loss, thus increasing the system efficiency. Electrical circuit of the proposed microinverter system, describing its primary functional components and power conversion stages is shown in Figure 2.

The primary DC power source of the system is a 600 W solar panel. Based on the estimated annual average solar irradiance of 650-750 W/m² in Villavicencio, the panel will supply an output of up to 400 W in real operation conditions. However, solar radiation is not constant over a day, significantly affecting energy generation. These variations shift the MPP, preventing the panel from being at its nominal capacity all the time, resulting in efficiency losses and the need for dynamic MPPT adjustments to optimize power extraction.

The designed system incorporates a step-up DC/DC voltage regulator with MPPT to deliver a stable and optimized output to the DC/AC converter. The MPPT controller, implementing the perturb and observe (P&O) algorithm, dynamically adjusts the duty cycle in order to track the MPP, maximizing energy extraction from the solar panel and enhancing system efficiency. This approach continuously compensates for irradiance variations, ensuring optimal performance. The following sections provide the assumptions and calculations for the regulator design.

A capability of supporting an input current of 14A is required in order to maximize energy transfer when the solar irradiance is typical. To realize a MPP voltage of 36 VDC, a boost regulator must be employed in order to increase the voltage to support effective power conversion. The regulator plays an important role in facilitating maximum power extraction from the PV panel and maintaining stable

output voltage. Figure 3 shows the topology of the boost regulator, which depicts its role in boosting system performance.

Table 1. Design bases

Characteristics	Value
Maximum power	500 W
Output	120 VAC / 4.1 A (pure wave 27 steps)
Input	15-36 VDC / 14 A

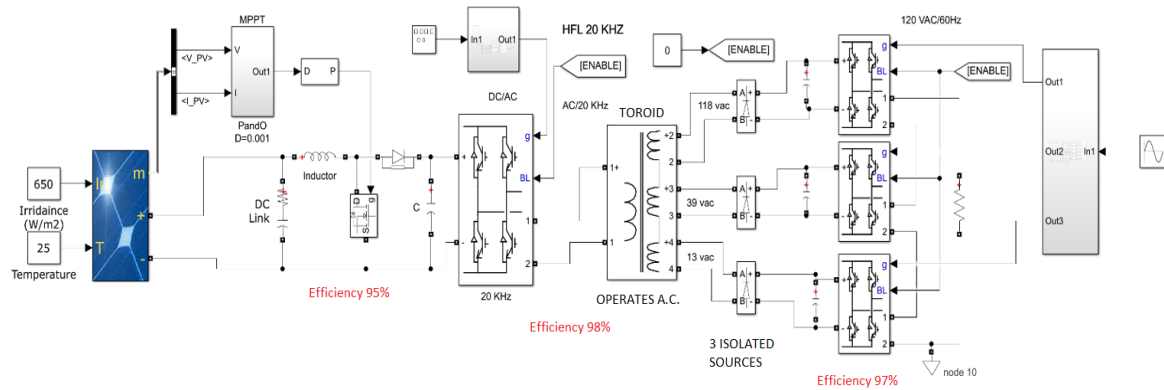


Figure 2. High-efficiency modular microinverter design

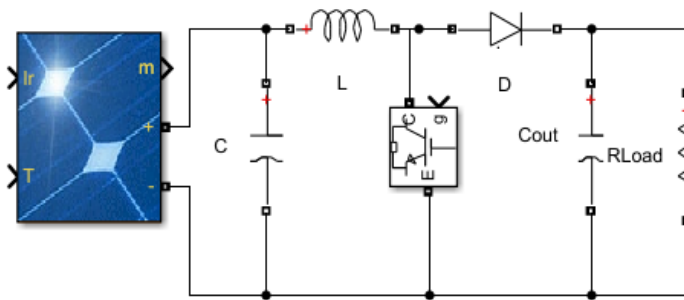


Figure 3. DC-DC boost regulator

By applying (1-7) from [25]-[26], the reference values for optimal MPPT operation are determined.

$$\frac{V_o}{V_s} = \frac{1}{1-D} \quad (1)$$

$$\frac{\Delta V_o}{V_s} = \frac{D}{RCf} \quad (2)$$

$$L_{min} = \frac{D(1-D)^2 R}{2f} \quad (3)$$

$$V_o = \frac{V_x}{1-D} \quad (4)$$

$$I_L = \frac{V_s}{(1-D)^2 R} \quad (5)$$

$$\frac{\Delta V_o}{V_o} = \frac{D}{RCf} \quad (6)$$

$$I_{max} = I_L + \frac{\Delta i_L}{2} = \frac{V_s}{(1-D)^2 R} + \frac{V_s D T}{2L} \quad (7)$$

A 20 kHz switching frequency is used to achieve smaller, low-cost components. The system employs MOSFET-based switching elements. To generate isolated DC sources, a transformer requiring an AC signal is necessary. This is accomplished through a HFL DC/AC converter; it switches the DC level at 20 kHz to generate a square-wave AC signal. The conversion process is performed by an H-bridge (HB) and a microcontroller that produces the necessary binary switching sequence. Operating at a high frequency reduces transformer size and enhances efficiency compared to low-frequency transformers. Likewise, passive components such as inductors and capacitors are minimized.

A key component of this design is the toroidal transformer, which generates three AC outputs. These outputs are combined through addition and subtraction to form a sine wave. To determine the different voltage levels, the primary winding's turns are calculated based on power and voltage. The secondary windings' turns are then computed, followed by rectification using Schottky diodes for high-frequency operation. Finally, the capacitor is sized to ensure an acceptable voltage ripple. In (8) and (9) define the turn calculations.

$$n_s = \frac{E_s}{4.44 * f * \Phi} \text{ (turns)} \quad (8)$$

$$C = \frac{1}{2fR \frac{\Delta V_o}{V_m}} \quad (9)$$

Here, E_s represents the voltage induced in the secondary winding (V), and fff denotes the frequency (Hz). Additionally, (10) and (11) are used to determine the winding areas:

$$SVP = np * \frac{Scup}{Fbp} \text{ (nm}^2\text{)} \quad (10)$$

Where, $SVP = Scup$ (for primary), and F_b is the winding spacing factor.

$$SVS = nS * \frac{Scus * Ces}{Fbs} \text{ (nm}^2\text{)} \quad (11)$$

Similarly, the next circuit component is the rectifier bridge and capacitor, which convert alternating current into direct current to supply each HB of the multilevel inverter. The input voltage waveform in the time domain is expressed by (12) [27]:

$$Vin = \sqrt{2} V1sen(wt) \quad (12)$$

Finally, to achieve a single-phase sinusoidal output of 120 VAC RMS at 60 Hz, a multilevel inverter was implemented. This inverter generates multiple voltage levels through binary combination. Figure 4 shows the sinusoidal waveform formed by the 27 generated levels:

The multilevel inversion technique constructs the sine wave by stacking voltage levels horizontally. Multilevel inverters use multiple power switches arranged to add or subtract voltages. Generating the wave requires determining the peak value, which is calculated using (13) and (14) [28]:

$$V_{RMS} = V_{pp} / \sqrt{2} \quad (13)$$

$$V_{pp} = V_{RMS} \times \sqrt{2} = 170 \quad (14)$$

The configuration of three HB enables the generation of 27 voltage levels, following the formula $3N + 1$, where N represents the number of auxiliary HB. Each HB requires an isolated DC voltage source to allow for voltage addition and subtraction. By solving (15) and (16) for this specific case, the following results are obtained:

$$V_{pp} = V_n + \frac{V_n}{3} + \frac{V_n}{9} \quad (15)$$

$$V_n = 118, \frac{V_n}{9} = 13 \text{ VDC} \quad (16)$$

$V_n/9$ represents the smallest voltage level used to construct the stepped sine wave, minimizing THD and eliminating the need for output filters. The implemented architecture features a series connection of three HB with different DC voltage levels, generating an AC output, as shown in Figure 5. This configuration employs an algorithm to control the binary switching of transistors, producing 27 voltage levels, each differing by 13 volts. By utilizing a 60 Hz sinusoidal reference signal, the system effectively replicates a sine wave.

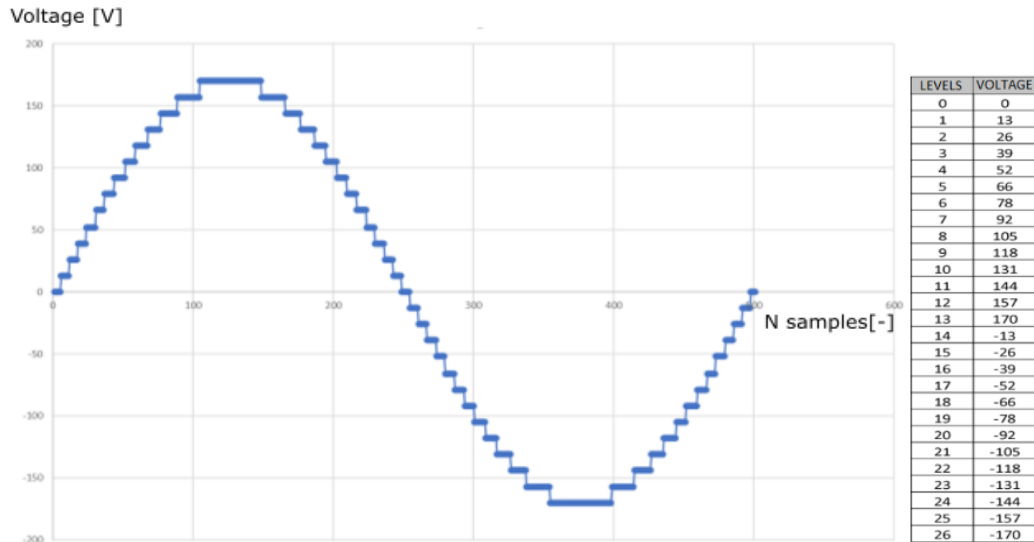


Figure 4. Multilevel signal generated by the combination of voltages of each HB

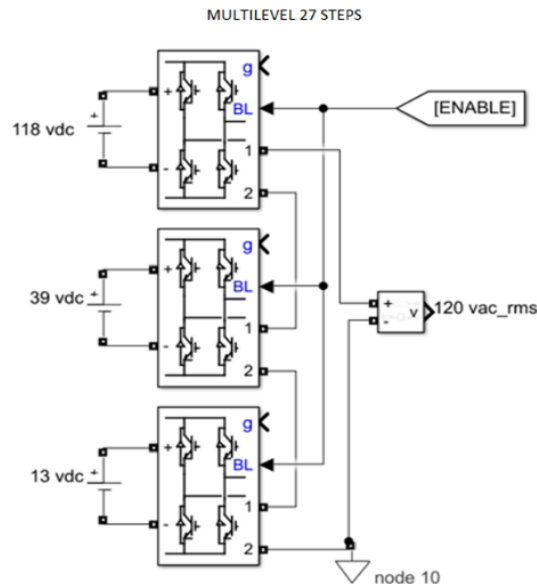


Figure 5. HB configuration for multilevel voltage generation of 27 steps

3. RESULTS AND DISCUSSION

Figure 6 shows the operation of the DC-DC boost regulator, maintaining a steady 36V DC output while dynamically adjusting current through MOSFET trigger control. The MPPT algorithm, utilizing the P&O method, continuously monitors power variations to maximize energy extraction from the solar panel. The boost converter's duty cycle is adjusted with a disturbance step size of 10 mW to ensure optimal power transfer. MATLAB simulations estimate an efficiency of 95% by comparing the solar panel's input power with the regulator's output power.

HB inverter performance, converting DC voltage into a pre-selected frequency 20 kHz square-wave AC signal is shown in Figure 7. High-frequency switching is the main feature of the HFL transformer application to provide multiple isolated AC voltage levels. Figure 8 confirms rectified DC voltage outputs achieved using the toroidal transformer and has a 97% efficiency level with ferrite core and low-impedance SiC switches. The multilevel inverter output waveform with a 27-level sinusoidal signal of THD of approximately 3%, significantly lower than in conventional inverters is shown in Figure 9. One of the key contributions of the proposed system is power quality improvement and harmonic reduction, which has excellent potential for future studies and high-end PV inverter applications.

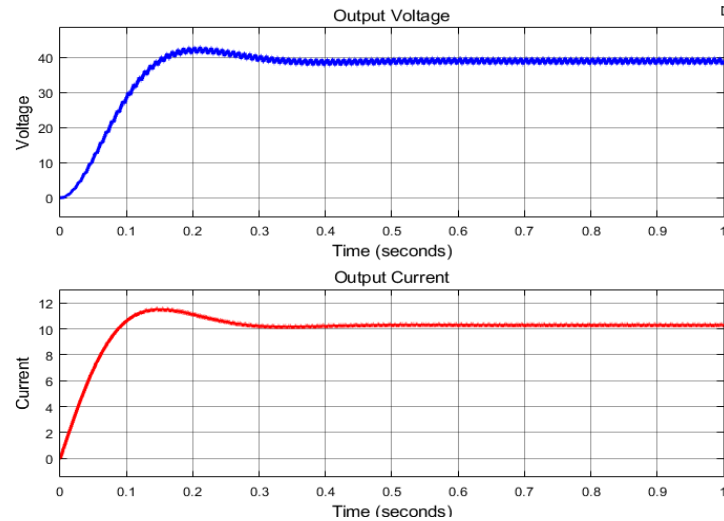


Figure 6. MPPT solar panel regulator output

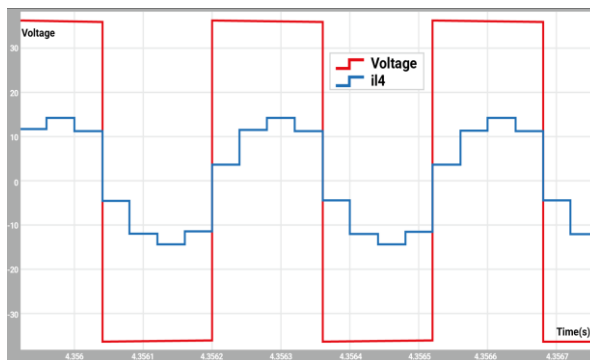


Figure 7. Inverter DC-AC HFL

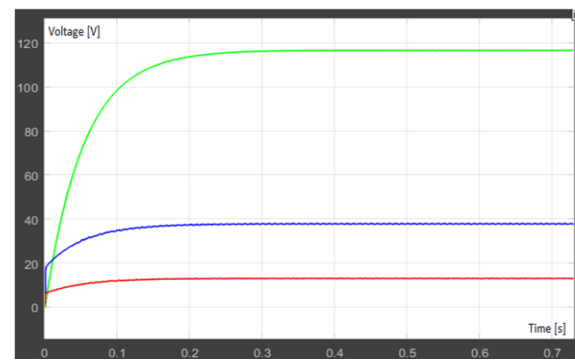


Figure 8. Isolated sources output

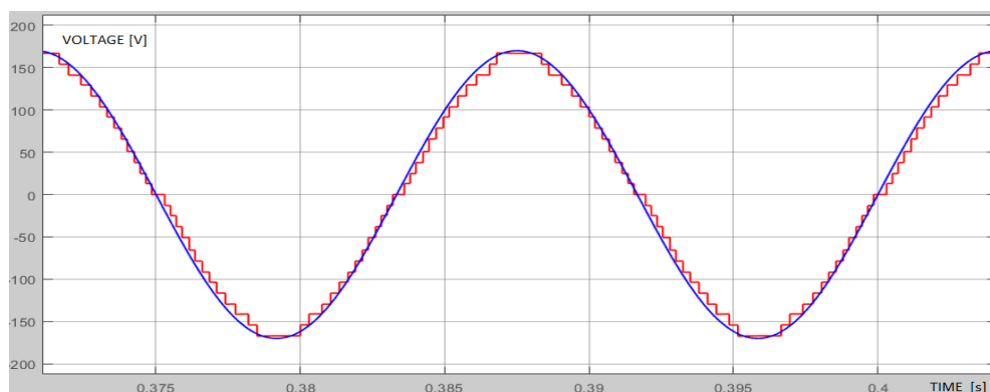


Figure 9. Multi-level inverter output

The proposed algorithm generates a multilevel sinusoidal signal by using a reference signal and a voltage level comparator [29]-[30], enabling the creation of 27 discrete voltage levels for the multilevel single-phase inverter. The system is designed for 97% efficiency by incorporating Silicon Carbide (SiC) MOSFETs, which offer low impedance in current saturation ($\sim 5 \text{ m}\Omega$) and minimal switching losses. Additionally, parallel operation of SiC MOSFETs can further enhance performance and efficiency. While these components are highly reliable-making them ideal for applications in military, aerospace, electric vehicles, UPS, and solar converters-their high cost remains a limiting factor for widespread adoption.

Figure 10 shows one of the key findings of this work, where power levels at the microinverter input and output are demonstrated. Efficiency calculation indicates that the system achieves an average efficiency of 90%, represented by the ratio of 330 W output power to 370 W input power. This result validates the excellence of the proposed design in energy conversion optimization and loss minimization, signifying its high-performance PV application potential.

Figure 11 shows the relationship between multilevel topology and waveform quality, in which a smaller number of levels results in increased THD, deteriorating power quality. Conversely, the rise in the number of voltage levels significantly enhances the precision of the waveform and reduces THD, resulting in improved overall system performance. The observation distinctly shows the linear dependence of multilevel inverter structure on harmonic elimination, justifying the requirement for inverters with higher levels for achieving improved power quality and efficiency of energy conversion systems.

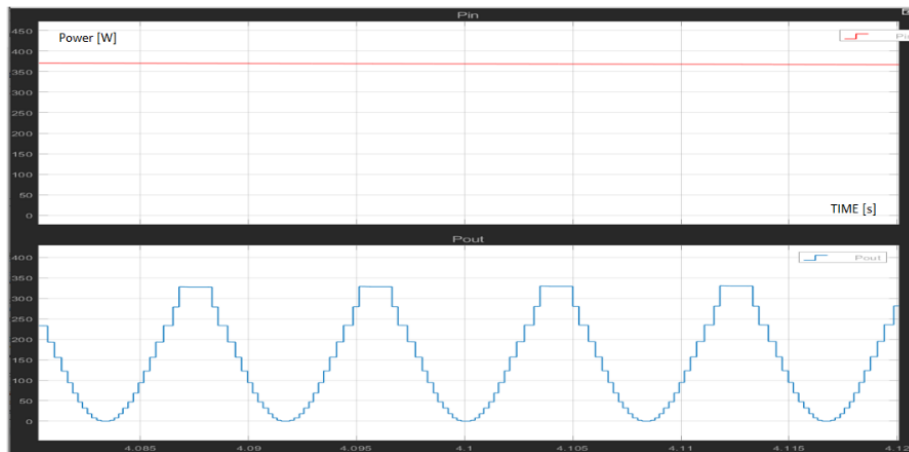


Figure 10. Microinverter power input and output

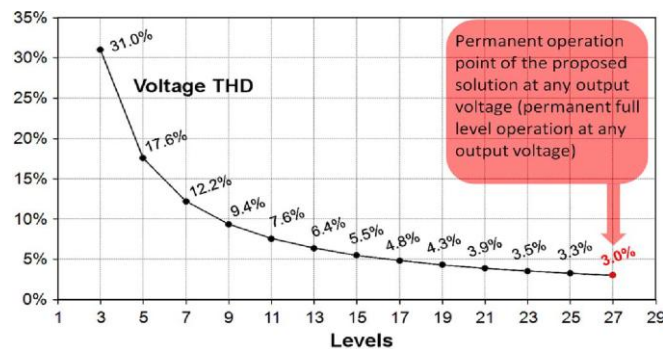


Figure 11. Experimental THD of the voltage as a function of the number of levels

4. CONCLUSION

The proposed high-efficiency microinverter system successfully integrates MPPT-controlled DC-DC conversion, HFL inverter, and multilevel inverter and has a overall efficiency of 90% with an output waveform of 3% THD. Synergy between MPPT algorithms, emerging semiconductor technologies, and optimal power electronics topology successfully enhances the solar energy conversion, demonstrating the advantages of high-frequency switching, voltage regulation, and elimination of harmonics, what could be taken into account in the different phases of scientific research related to microinverter. These results validate the effectiveness of multilevel inverters and high-frequency conversion in improving the power quality and system performance.

Silicon Carbide (SiC) transistors' application results in improved switching efficiency, lower conduction losses, and improved thermal performance and hence render them a critical component in high-power-density applications. However, SiC device cost remains a limiting factor for mass deployment. Hybrid solutions that are cost-effective, wherein Si-based and SiC-based switches are combined, could be conceived

in the future to marry efficiency with cost-effectiveness and render high-performance PV inverters economically viable.

High-frequency conversion plays a crucial role in minimizing the size of passive components such as transformers, inductors, and capacitors, where it is concluded that the design principles of usability and user experience. This reduction leads to a more compact and cost-effective design. By operating at higher frequencies, the system enhances efficiency while decreasing material usage, making it an optimal solution for modern power conversion applications.

By operating at high frequencies, the system gives low energy losses, reduced component size, and improved overall power density, and as such, the system is well suited for PV distributed applications. Moreover, with the implementation of advanced modulation techniques, for example, space vector modulation (SVM) or selective harmonic elimination (SHE), waveform synthesis and switching efficiency may be enhanced even further. The study also identifies module-level MPPT control as a requirement, which can optimize individual panel performance independently and mitigate mismatch losses due to partial shadowing or non-uniform panel aging. Microinverters provide better fault detection, improved monitoring, and improved scalability than centralized inverter architectures. Microinverters are therefore a superior option for residential, commercial, and industrial solar applications.

Future research will focus on integrating real-time adaptive control techniques and machine learning-based MPPT algorithms to improve dynamic tracking capability under sudden environmental variation. Additionally, the use of soft-switching techniques and optimized transformer core materials will lead to higher efficiency and lifetime. All the improvements make the proposed microinverter an advanced technology for efficient, scalable, and high-performance solar energy conversion.

ACKNOWLEDGMENTS

The authors thank to Universidad de los Llanos and Specialization in Instrumentation and Industrial Control for their support in the development of this project.

FUNDING INFORMATION

Product financed by the authors.

AUTHOR CONTRIBUTIONS STATEMENT

This journal uses the Contributor Roles Taxonomy (CRediT) to recognize individual author contributions, reduce authorship disputes, and facilitate collaboration.

Name of Author	C	M	So	Va	Fo	I	R	D	O	E	Vi	Su	P	Fu
Naranjo Lourido Walter	✓	✓	✓	✓	✓	✓		✓	✓	✓			✓	✓
Sanchez Fierro Jhon Manuel		✓	✓	✓	✓	✓	✓	✓	✓	✓	✓	✓	✓	✓
Monroy Cadena Diana Paola		✓	✓	✓	✓	✓	✓	✓	✓	✓	✓	✓	✓	✓
Martinez Baquero Javier Eduardo	✓	✓		✓	✓	✓	✓			✓	✓	✓	✓	✓

C : **C**onceptualization

M : **M**ethodology

So : **S**oftware

Va : **V**alidation

Fo : **F**ormal analysis

I : **I**nvestigation

R : **R**esources

D : **D**ata Curation

O : Writing - **O**riginal Draft

E : Writing - Review & **E**editing

Vi : **V**isualization

Su : **S**upervision

P : **P**roject administration

Fu : **F**unding acquisition

CONFLICT OF INTEREST STATEMENT

The authors state no conflict of interest.

INFORMED CONSENT

Not applicable as it requires the involvement of personnel from outside the work team, no sensitive information was handled.

ETHICAL APPROVAL

Not applicable in the research

DATA AVAILABILITY

The data that support the findings of this study are available from the corresponding author, [W.N.L.], upon reasonable request.





REFERENCES

- [1] V. P. Markevich *et al.*, "Recombination centers resulting from reactions of hydrogen and oxygen in n-type Czochralski silicon," in *2017 IEEE 44th Photovoltaic Specialist Conference, PVSC 2017*, Jun. 2017, pp. 2025–2030, doi: 10.1109/PVSC.2017.8366092.
- [2] C. García and M. Montero, "Toma de decisiones, valores y factores contextuales, su relación con el consumo de energía eléctrica," *Quaderns de psicologia. International journal of psychology*, vol. 15, no. 2, pp. 39–54, 2018.
- [3] E. Monagas, B. Palacios, and M. Rueda, "Análisis de la estabilidad transitoria de un sistema de generación y transmisión de energía eléctrica. caso Electricidad de Valencia–Corpoelec," *Revista Ingeniería UC*, vol. 17, no. 3, pp. 57–67, 2010.
- [4] X. Lei, J. Liu, L. Du, and L. Zhang, "Analysis on large consumer price models in electricity market," in *3rd International Conference on Deregulation and Restructuring and Power Technologies, DRPT 2008*, Apr. 2008, pp. 426–430, doi: 10.1109/DRPT.2008.4523444.
- [5] Y. Zhang, Q. Zhou, L. Zhao, Y. Ma, Q. Lv, and P. Gao, "Dynamic Reactive Power Configuration of High Penetration Renewable Energy Grid Based on Transient Stability Probability Assessment," in *2020 IEEE 4th Conference on Energy Internet and Energy System Integration (EI2)*, Oct. 2020, pp. 3801–3805, doi: 10.1109/EI250167.2020.9346594.
- [6] D. Mooney and B. Kroposki, "Electricity, resources, and building systems integration at the national renewable energy laboratory," in *2009 IEEE Power and Energy Society General Meeting, PES '09*, Jul. 2009, pp. 1–3, doi: 10.1109/PES.2009.5275358.
- [7] I. J. Hashim, "A New Renewable Energy Index," in *2021 6th International Conference on Renewable Energy: Generation and Applications, ICREGA 2021*, Feb. 2021, pp. 229–232, doi: 10.1109/ICREGA50506.2021.9388297.
- [8] S. Paul, T. Dey, P. Saha, S. Dey, and R. Sen, "Review on the development scenario of renewable energy in different country," in *2021 Innovations in Energy Management and Renewable Resources, IEMRE 2021*, Feb. 2021, pp. 1–2, doi: 10.1109/IEMRE52042.2021.9386748.
- [9] M. G. Tyagunov and T. Y. Min, "Analysis of ways of solving the problem of hybrid energy complexes based on reserve for power supply of autonomous rural consumers in Myanmar," in *3rd Renewable Energies, Power Systems and Green Inclusive Economy, REPS and GIE 2018*, Apr. 2018, pp. 1–6, doi: 10.1109/REPSGIE.2018.8488852.
- [10] T. Gupta, G. K. Pandit, B. Sharan, H. Mishra, S. Singh, and R. Dewan, "A Robust Approach for Analysis and Visualization of CO₂ and Greenhouse Gas Emission and Its Effect," in *2023 10th International Conference on Computing for Sustainable Global Development (INDIACom)*, 2023, pp. 238–243.
- [11] K. H. Yang, H. Yoe, J. D. Ahn, and M. H. Lee, "Study on a Data Collection Platform for Greenhouse Gas Emission Factors in Smart Farms for Low-Carbon Agriculture," in *2025 International Conference on Artificial Intelligence in Information and Communication (ICAIIIC)*, 2025, pp. 1065–1068. doi: 10.1109/ICAIIIC64266.2025.10920795.
- [12] W. Wu, C. Zhang, J. Su, and H. Wang, "The Design of New High Efficiency Photovoltaic Grid and Independent Power Supply Inverter," in *2015 International Conference on Computational Intelligence and Communication Networks (CICN)*, Dec. 2015, pp. 1579–1582, doi: 10.1109/CICN.2015.300.
- [13] R. Dhivya, K. Jaiganesh, and K. Duraiswamy, "Performance analysis of boost half bridge photovoltaic microinverter using RCC variable step size algorithm," in *2013 International Conference on Renewable Energy and Sustainable Energy (ICRESE)*, Dec. 2013, pp. 75–80, doi: 10.1109/ICRESE.2013.6927791.
- [14] W. J. Cha, Y. W. Cho, J. M. Kwon, and B. H. Kwon, "Highly efficient microinverter with soft-switching step-up converter and single-switch-modulation inverter," *IEEE Transactions on Industrial Electronics*, vol. 62, no. 6, pp. 3516–3523, 2015, doi: 10.1109/TIE.2014.2366718.
- [15] O. Haris, A. Darmawan, and A. Juliansyah, "Efficiency Analysis of Using Solar Panel System Tracker to Static Solar Panel," in *7th International Conference on Computing, Engineering and Design, ICCED 2021*, Aug. 2021, pp. 1–6, doi: 10.1109/ICCED53389.2021.9664841.
- [16] T. Esram and P. L. Chapman, "Comparison of Photovoltaic Array Maximum Power Point Tracking Techniques," *IEEE Transactions on Energy Conversion*, vol. 22, no. 2, pp. 439–449, Jun. 2007, doi: 10.1109/TEC.2006.874230.
- [17] G. H. Min, K. H. Lee, J. I. Ha, and M. H. Kim, "Design and Control of Single-Phase Grid-Connected Photovoltaic Microinverter with Reactive Power Support Capability," in *2018 International Power Electronics Conference, IPEC-Niigata - ECCE Asia 2018*, May 2018, pp. 2500–2504, doi: 10.23919/IPEC.2018.8507578.
- [18] L. Ruiz C., J. Beristáin J., I. Sosa T., and J. Hernandez L., "Maximum Power Point Tracking Algorithm Study Disturb and Observe," *Journal of Electrical, Electronic and Computer Engineering (RIEE&C)*, vol. 8, no. 1, pp. 17–21, 2010, [Online]. Available: https://www.itson.mx/publicaciones/rieeec/Documents/v8/art3vf_estudio_del_algoritmo_de_seguimiento_de_punto_de_maxima_potencia_perturbar_y_observar.pdf.
- [19] M. Kaczmarek, R. Nowicz, and A. Szczesny, "Equivalent circuit parameters of the current transformer with toroidal core in conditions of distorted signals transformation," *Proceedings - International Symposium: Modern Electric Power Systems, MEPS'10*, pp. 1–5, 2010.
- [20] Departamento Administrativo de la Función Pública, "Decreto 829 de 2020." Función Pública, Bogotá, pp. 1–6, 2020. [Online]. Available: <https://www.funcionpublica.gov.co/eva/gestornormativo/norma.php?i=127884>
- [21] D. A. B. Zambra, C. Rech, and J. R. Pinheiro, "Comparison of Neutral-Point-Clamped, Symmetrical, and Hybrid Asymmetrical Multilevel Inverters," *IEEE Transactions on Industrial Electronics*, vol. 57, no. 7, pp. 2297–2306, Jul. 2010, doi: 10.1109/TIE.2010.2040561.
- [22] S. Chiniforoosh *et al.*, "Definitions and Applications of Dynamic Average Models for Analysis of Power Systems," *IEEE Transactions on Power Delivery*, vol. 25, no. 4, pp. 2655–2669, Oct. 2010, doi: 10.1109/TPWRD.2010.2043859.
- [23] J. Frau, "Efficiency in transformers. II International Conference on Energy Innovation-University of Catalaunya, 2006." <https://resources.altium.com/es/p/isolated-vs-non-isolated-power-supplies-right-choice-without-fail>. (accessed Feb. 06, 2015).
- [24] R. J. Leonardo and A. González, "Design procedure for low voltage current transformers with toroidal core," Diploma work, 2017.





- [25] A. Dmowski and T. Dzik, "Electronics And Power Electronics Devices In Dissipated Power Systems With Fuel Cells," in *2007 Compatibility in Power Electronics*, May 2007, pp. 1–9, doi: 10.1109/CPE.2007.4296507.
- [26] X. Shi, S. Filizadeh, and L. Wang, "Analysis of Submodule Capacitor Voltage Ripple and Second-Harmonic Current in MMCs," in *2019 20th Workshop on Control and Modeling for Power Electronics (COMPEL)*, Jun. 2019, pp. 1–8, doi: 10.1109/COMPEL.2019.8769665.
- [27] X. Wu, C. Xiong, F. Diao, and Y. Zhang, "Modularized Model Predictive Control Scheme with Capacitor Voltage Balance Control for Single-Phase Cascaded H-bridge Rectifier," in *2018 IEEE Energy Conversion Congress and Exposition, ECCE 2018*, Sep. 2018, pp. 4021–4023, doi: 10.1109/ECCE.2018.8558457.
- [28] S. Ahmad, I. Khan, A. Iqbal, and S. Rahman, "A Novel Pulse Width Amplitude Modulation for Elimination of Multiple Harmonics in Asymmetrical Multilevel Inverter," in *2021 IEEE Texas Power and Energy Conference, TPEC 2021*, Feb. 2021, pp. 1–6, doi: 10.1109/TPEC51183.2021.9384988.
- [29] C. Summatta and T. Phurahong, "Three-Stage Window Comparator Circuit with MOSFET-Resistor Voltage Reference," in *2020 3rd International Conference on Power and Energy Applications, ICPEA 2020*, Oct. 2020, pp. 37–40, doi: 10.1109/ICPEA49807.2020.9280156.
- [30] C. Summatta, T. Phurahong, W. Rattanangam, and W. Chaiyong, "Low-cost and Compact Window Comparator Circuit with MOSFET-Resistor Voltage References," in *2019 IEEE 2nd International Conference on Power and Energy Applications, ICPEA 2019*, Apr. 2019, pp. 75–78, doi: 10.1109/ICPEA.2019.8818512.

BIOGRAPHIES OF AUTHORS







Walter Naranjo Lourido     holds a PhD. In Electronics Engineering from Universidad de Los Andes, Colombia. He was a postdoctoral research engineer at the Pontificia Universidad Católica, Santiago, Chile. He explores new power M2C topologies related to fast and ultra-fast DC chargers for electric vehicles. This research was funded by the National Agency of Research and Development (ANID) in Chile. His research interests are power electronics, vehicle electrification, design of powertrains, energy efficiency, and microgrids. He can be contacted at email: wnanranjo@unillanos.edu.co.







John Manuel Sanchez Fierro     is an Electronic Engineer graduated from Universidad de los Llanos in 2004. Posgraduated in Project Management at Universidad Minuto de Dios in 2014, posgraduated in Instrumentation and Industrial Control at Universidad de los Llanos in 2021. His current working as engineer design for the oil&gas sector on Instrumentation, Automation and Control. He can be contacted at email: john.sanchez.fierro@unillanos.edu.co.



Diana Paola Monroy Cadena     is an Industrial Engineer graduated from Universidad del Meta in 2017, posgraduated in Instrumentation and Industrial Control at Universidad de los Llanos in 2021. She is currently studying programming at Universidad del Norte. She can be contacted at email: diana.monroy@unillanos.edu.co.



Javier Eduardo Martinez Baquero     is an Electronic Engineer graduated from Universidad de los Llanos in 2002. Posgraduated in Electronic Instrumentation from Universidad Santo Tomas in 2004, posgraduated in Instrumentation and Industrial Control at Universidad de los Llanos in 2020 and Msc in Educative Technology and Innovative Media for Education at Universidad Autonoma de Bucaramanga in 2013. His current working as associated professor of Universidad de los Llanos and research focuses on Instrumentation, Automation, Control and Renewable Energies. He can be contacted at email: jmartinez@unillanos.edu.co.